https://doi.org/10.31256/If9Ru3F

Gliding Mechanism with Hinged Aeroelastic Wings

Jingcheng Sun, Junfeng Yang, Robert Richardson and Chengxu Zhou

***Abstract*—Last few decades have seen a rising number of robot designs combining jumping and gliding functions. Engineers have drawn inspirations from birds for efficient gliding , namely their body morphology and flying techniques. Devices that are inspired by birds have benefited aircraft designs with the most prominent of them being the winglet. This work presents a glider design that can be coupled with jumping robots for locomotion and is able to have efficient and stable flights. A aeroelastic hinged winglet design is added to the glider, which enables the wings to have load alleviation capabilities.**

***Index Terms*—gliding robots, jumping robots, wingtip devices, aerodynamics**

I. Introduction

In the past decade, there have been an increasing number of designs combining jumping and gliding on a single robot. The function of the gliding constituent is usually enabling the robot with efficient flight. The EPFL jumpglider [1], for example, manages to achieve equilibrium flight with constant speed during their gliding phase. When it glides, the trajectory shows a clear leveled or even climbing flight section due to induced lift after it gains airspeed. The theoretically best design for gliders to have long and stable flights could be found in existing sailplanes. F. Thomas did thorough research on the sailplane design in the past century and provided basic mathematical theories to calculate the equilibrium airspeed and sink speed of aircraft given specifications [2]. In his paper, it is mentioned that the preferred properties of the sailplanes are high lift coefficient and high aspect ratio. These properties help the plane to gain a lower sink speed to travel larger distance with limited altitude loss.

Inspirations also exist in nature. Some species of birds cup their wings during gliding and diving. Gowree *et al.* analyzed the vortices around the body of peregrine falcons during flight [3] and found that there is an absence of wingtips vortices in the cupped shape and thus it has lower induced drag. A similar phenomenon with the same name can be found on airplanes as a large source of induced drag. Engineers have come up with ways to reduce the wing-tip vortices and the most widely used one is the winglet. Airbus designed airplane, AlbatrossOne, utilizes semi aeroelastic hinged wingtip devices [4]. The winglets are connected by hinges with their movements elastically constrained. The main purpose of the hinged wingtips is load alleviation as they can respond to severe gusts and maneuvers by not transmitting bending moment.

Authors are with the School of Mechanical Engineering, University of Leeds, UK. c.x.zhou@leeds.ac.uk

This work was supported by the EPSRC [grant numbers EP/V026801/2, EP/W002299/1] and the AMPI [Innovate UK project number 84646].

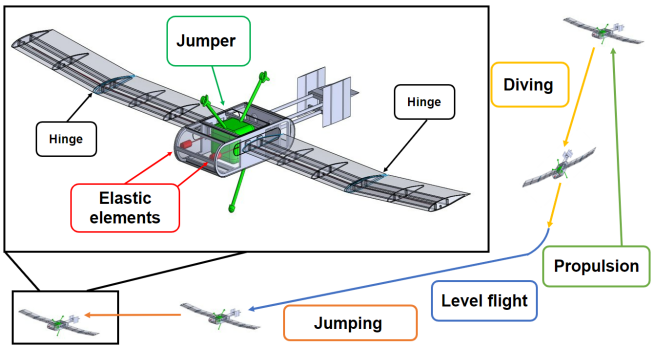

Fig. 1. The 4 phases of locomotion and the glider over view. The green part is a jumper that can be detached while the spring mechanism is in red. The glider dives to gain the airspeed required for level flight. The jumper starts working once it lands.

Therefore, design strategies are drawn in this work for a small-scale glider to fly efficiently according to the findings in the mentioned papers. The design goals are: high glide and aspect ratios; light weight; a load alleviation mechanism to protected the frame due to material cut and to minimize structural morphing. They are detailed in the following sections.

II. Glider Design Overview

This work presents a gliding mechanism that can be coupled with jumping robots to create a jump-glider. The planned trajectory and functions are shown in the illustration (Fig. 1). The glider will usually be propelled to an elevated position before going into a glide. Jumping will take over as the locomotion method once it reaches the ground. Equilibrium gliding can be modeled by [2]:

$$V = \sqrt{\frac{2W}{\rho \times S \times C_l}}, \qquad V_s = (C_d/C_l)V, \tag{1}$$

where V is the forward speed, W is the weight of the glider, ρ is the density of air, S is the reference area of the wing, C_l is the lift coefficient, C_d is the drag coefficient and V_s is the sink speed of the glider.

Glide ratio (C_l/C_d) describes not only the ratio of forward speed and sink speed but also that of ground distance traveled and loss of altitude. Assuming a descent of 5 m after the glider enters level flight, it can theoretically travel for more than 300 m (compared to EPFL with a glide ratio of about 2.3). The design strategy is to maximize the glide ratio and wing area so that the gliding distance can be long with limited descent and the equilibrium gliding speed is attainable at the same time. The wing profile is based on the airfoil HQ2.0 whose properties are shown in Table I at an angle of attack of 5°

TABLE I
SUMMARY OF THE WING PARAMETERS AND CALCULATED SPEEDS

Wingspan (m)	$S\ (m^2)$	C_l	(C_l/C_d)	$V\ (m/s)$	$V_s\ (m/s)$
0.9	0.09	0.8133	72	4.6	0.064

TABLE II
RISE ANGLES VERSUS THE BENDING MOMENTS, STRESSES AND DISPLACEMENT (URES) WITH INPUT LOAD INCLUDED.

Angles (°)	Bending moment (Nm)	von Mises (MPa)	URES at the tip (cm)	L_1 (N)	L_2 (N)
0 (fixed)	1.923	22.76	9.10	4.7	3.8
45	1.644	20.45	7.81	–	–
90 (released)	0.9725	11.90	3.45	–	–

(data from airfoil tools). The equilibrium forward speed and sink speed are calculated in Table I using (1).

III. WING MECHANISM

The large wingspan of the glider could be a problem to the structural integrity when there is turbulence in the air since the material use of the frame was minimized to cut weight. Thus, the hinged aeroelastic wing design is proposed specifically for load alleviation and countering this problem. The winglets are connected to the main body of the wings by a spring mechanism (red line in a, c and e in Fig. 2) with a string going through inside of the wings guided by pulleys and ending at an elastic element in the fuselage. The spring constant of the elastic element is set to a value so that the regular level gliding speed in calm air will cause a $5°$ rise for the winglet to create the dihedral effect and further improve the stability of flight. Additionally, the winglets can be released from spring tension and form a $90°$ angle to the main body.

The lift force acting on the main body and the winglet will be called L_1 and L_2, respectively. They can be calculated as

$$L_{1,2} = \frac{1}{2}\rho V^2 S_{1,2} C_l, \tag{2}$$

where S_1 and S_2 are the reference areas of the wing main body and the winglet. As we assume the $5°$ rise angle at the equilibrium speed of 4.6 m/s, the spring stiffness is chosen as 1.96×10^{-3} Nm per degree. Thus, when the winglet has a $45°$ rise, L_1 is 3.8 N. Then, the speed of the turbulence can be obtained using (2), and the result is 19.5 m/s.

The following equation is the theoretic estimation of the bending moment M at the root of the wings:

$$M = bL_1 + (l\cos\theta + a)L_2, \tag{3}$$

where θ is the rise angle of the winglet, b is the distance between the wing root and the aerodynamic centre of the main body, l is the length of the main body and a is the distance between the hinge and the aerodynamic centre of the winglet. The results are presented in Table II.

Finally, a finite element analysis was done on the wing frames to assess the stress-deformation status with the wing roots fixed and loads being calculated lifts (L_1 & L_2) acting normally on the aerodynamic centres of main body and

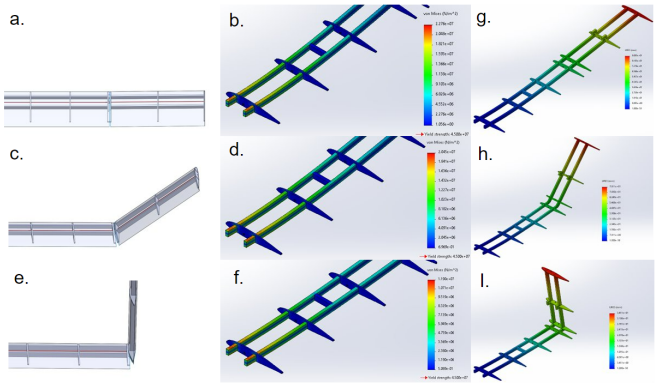

Fig. 2. Pictures a, c and e are illustration of the wings at angles 0°, 45°and 90°; while b, d and e are their corresponding simulation results showing the distribution of stress.The additional images g, h and i are the displacements of the structure under said stresses.

winglet. The element size was meshed to be 1.54 mm with the area around the wing root to be extra fine (1.0 mm). As shown in Fig. 2, the maximum von Mises stress which only concentrates at the wing root decreased from 22.76 MPa at $0°$ (fixed with no spring) to 20.45 MPa at $45°$. When the hinge is released, the stress drops 47.7% to 11.9 MPa which is roughly a quarter of the yield strength (45 MPa). The displacement at the wingtip has reductions of 14.2% and 62.1% at $45°$ and $90°$, respectively. The reduction in displacement is as important as stress since the deformation of the material is relatively large due to the thin nature of the structure. Significant morphing of the wing may change its aerodynamic behavior and increase the difficulty of flight trajectory planning.

IV. CONCLUSION

A novel gliding mechanism that can be coupled with jumping robots is introduced in this paper. The profile and the aspect ratio of the basic wing was designed so that the glider is able to have long and efficient flights. The aeroelastic hinged winglets provide a natural stabilizing factor to the glider as well as being able to released from spring tension to alleviates load on the wing when the protection provided by the elasticity is not sufficient.

For future work, computational fluid dynamics study should be done in order to validate the calculations using estimated data. A prototype should be built and tested in real-world scenarios. Furthermore, a control system should be developed for the glider to achieve self-flight inside of rely on manual remote control.

REFERENCES

[1] M. Kovač, *et al.*, "The EPFL jumpglider: A hybrid jumping and gliding robot with rigid or folding wings." IEEE International Conference on Robotics and Biomimetics, 2011.

[2] F. Thomas, "1OO Years of sailplane design and beyond." Technical Soaring, 2003.

[3] E. Gowree, *et al.*, "Vortices enable the complex aerobatics of peregrine falcons." Communications Biology, 2018.

[4] T. Wilson, *et al.*, "Small scale flying demonstration of semi aeroelastic hinged wing tips." International Forum on Aeroelasticity and Structural Dynamics, 2019.